Journal of Materials Chemistry A

COMMUNICATION

View Article Online
View Journal | View Issue

Cite this: J. Mater. Chem. A, 2016, 4, 2408

Received 16th November 2015
Accepted 18th January 2016

DOI: 10.1039/c5ta09209d

www.rsc.org/MaterialsA

Self-healing fluoropolymer brushes as highly polymer-repellent coatings†

Zhanhua Wang[ab] and Han Zuilhof*[bc]

The fouling of surfaces by organic polymers can be strongly reduced by applying a 75 nm covalently bound fluorinated polymer brush onto the surface. This strong reduction can be repaired, even more than 10 times, after the polymer brush has been damaged (*e.g.* by a strong base) using the self-repairing character of these brushes *via* molecular reorganization at the surface–air interface at slightly elevated temperatures.

The fouling of surfaces by biological entities (from isolated proteins and other biopolymers to entire organisms) has been studied in great detail.[1,2] This has led to a deep understanding of at least the initial stages of biofouling[3] and the design of novel materials that successfully repel such fouling.[4] Probably the best known examples are the first-generation antifouling polyethylene oxide polymers[5] and the current state-of-the-art zwitterionic polymer brushes.[6,7] Such progress has been nearly fully absent in the field of fouling by polymers[8] in non-aqueous, organic media.[9] Such fouling is of significant industrial importance,[10,11] *e.g.* in food processing, paper manufacturing, and high-resolution 3D printing. Yet, there are only very few literature studies on this topic that probe the mechanisms behind it down to a molecular level.[12]

Recently, we reported the first systematic study of the fouling of high-quality fluorinated monolayers onto ultraflat Si surfaces by a wide range of polymers with variable molecular weights.[13] This choice was based on the high degree of control that is available in the construction of such monolayers, whereas ultraflat substrates rigorously decouple the contributions of the molecular structure and surface roughness. In addition, the choice of Si was practically driven by the fact that small-scale orifices used in industry are increasingly lithographically prepared from Si. Fouling over time by polymers therefore limits their long-term use. In this first study we found that partially fluorinated monolayers, especially mono-fluoro alkyne-derived Si–CH=CH–$C_{13}H_{28}CH_2F$ monolayer **F1**, showed excellent antifouling behavior against a range of polymers with different molecular weights even on atomically flat Si surfaces. However, while extremely successful for most of the tested polymers, in two regimes limitations were observed. First, for a variety of polymers, fouling was still observed in solvents of low polarity. Second, for a special polymer P2VP, heavy fouling was also found on the **F1** monolayer due to the strong interaction between the single C–F bond and the protonated N atom in P2VP. Finally, a generic limitation of organic monolayers is their susceptibility to mechanical damage and the absence of self-repair. Self-repair is a highly desirable property,[14–16] and significant successes in the field of self-repairing and anti-fouling surface have been achieved by *e.g.* the groups of Aizenberg (based on liquid captured within nanostructures),[17] Minko (using flexible polymers),[18] Sun (using layer-by-layer assembled films),[19] and Zeng (using catechol-mediated hydrogen bonding interactions and aromatic interactions).[20] Challenges still in this field are the evaporation of the infused liquid, the necessity of complicated fabrication of the required micro/nano structures or the limitation to use in an aqueous environment, use of preferably ultrathin surface coatings, and overall: the full repair of surface properties. Therefore, long-term anti-fouling coatings with a self-healing function pre-incorporated inside the materials by facile methods that can be widely used still deserve significant attention.[21,22]

In the current communication we aim to address all these issues by the development of a covalently grafted fluoropolymer brush (75 nm thickness) onto atomically flat Si(111) surfaces using atom transfer radical polymerization (ATRP; Fig. 1a). The surface functionalization and initiator immobilization were achieved by standard methods onto atomically flat, oxide-free Si(111) surfaces, and the resulting surfaces – like all surfaces

[a]Material Innovation Institute (M2i), Elektronicaweg 25, 2628 XG Delft, The Netherlands

[b]Laboratory of Organic Chemistry, Wageningen University Dreijenplein 8, 6703 HB Wageningen, The Netherlands. E-mail: han.zuilhof@wur.nl

[c]Department of Chemical and Materials Engineering, King Abdulaziz University, Jeddah, Saudi Arabia

† Electronic supplementary information (ESI) available: Details of polymer brush synthesis, contact angle and surface coverage. See DOI: 10.1039/c5ta09209d

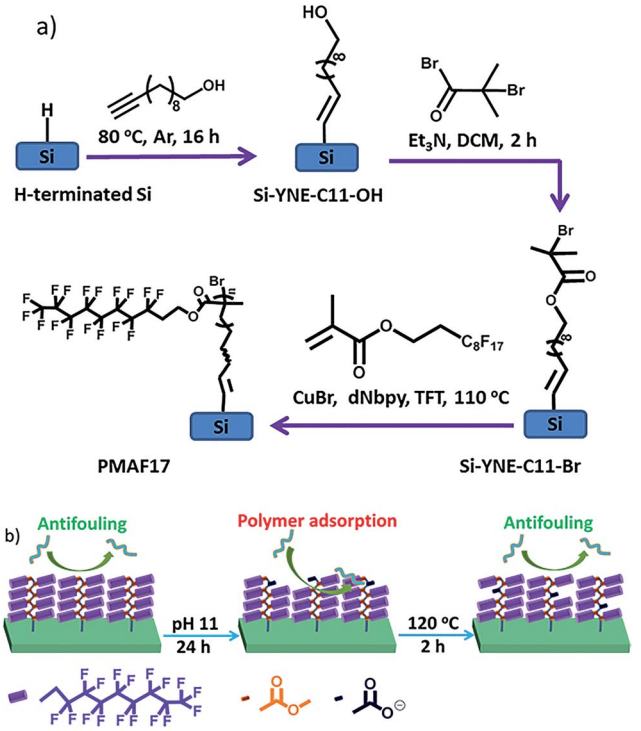

Fig. 1 (a) Preparation of the fluoropolymer brush on Si(111). (b) Schematic illustration of the antifouling behavior of the original, damaged and repaired **PMAF17** brush upon immersion into a polymer solution.

under study – were characterized in detail by static water contact angle (CA) and X-ray photoelectron spectroscopy (XPS) (Table S1 and Fig. S1†). Next, the poly(2-perfluorooctylethyl methacrylate) (**PMAF17**) brush was grafted to a carefully controlled thickness (75 nm) onto the initiator-immobilized Si surface *via* surface-initiated ATRP.[23] This polymer brush was selected because of its high hydrophobicity (CA = 121°) and ultra-low surface energy.[24] In addition, rearrangement of the polymer segments above the glass transition temperature (T_g) of the **PMAF17** brush (T_g of bulk **PMAF17** = 40 °C) was hypothesized to induce the fluorinated tail to come to the top of the surface to decrease the surface interaction between the brush and air. This property will endow the **PMAF17** brush with a self-healing character, due to the reregulating chemical composition at the surface *via* the movement of the polymer segments (Fig. 1b). Furthermore, such covalent grafting endows fluoropolymer brushes with an improved stability and durability.

The brush-coated surface is rather flat, as displayed by a low surface roughness (see below: RMS = 0.87 nm, Fig. 4C1), compared to its thickness (75 nm). This thickness was chosen as an optimum between two opposing trends: on the one hand ultrathin coatings will be most conformal to surface structures, and be useful on nanopatterned surfaces without effectively removing that structuring. On the other hand we reasoned that a minimal thickness is required, as only for polymer coatings with a thickness >*ca.* 50 nm we expected the fluoropolymer brush to possess roughly the same T_g as the corresponding bulk

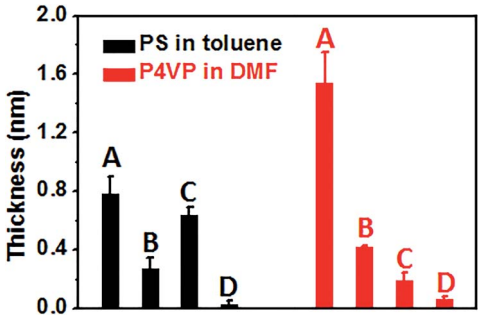

Fig. 2 XPS-determined polymer surface fouling upon immersion into PS–toluene (left/black) and P2VP–DMF (right/red) solutions for 12 h. (A) Unmodified Si; (B) **F1** monolayer; (C) **F17** monolayer; (D) **PMAF17** brush.

polymer.[25,26] This means that above this threshold thickness the thermo-induced movement of the polymer brush is independent of the substrate, which is favored for the self-healing process. Furthermore, the thicker the polymer brush, the more times the brush can be repaired, eventually leading to longer service lifetimes. Making thicker **PMAF17** brushes is trivial by using *e.g.* longer reaction times in the polymerization step, so the challenge is in getting polymer layers as thin as possible while still displaying this character. Finally, we chose the two most rigorously fouling conditions found in our previous study[13] PS in highly apolar toluene and strongly interacting P2VP in DMF as two model systems to study the antifouling properties of the **PMAF17** brush. Unmodified silicon surfaces, and hexadecenyl monolayers with one (**F1**) or 17 fluorine atoms (Si–CH=CH–C_6H_{12}–C_8F_{17}; **F17**) (see Scheme S1†) were used as references.

To study the polymer antifouling properties, modified surfaces were dipped overnight in a solution containing the polymer, taken out, and cleaned with the same solvent (Fig. 1). The polymer fouling was studied by XPS, CA and a previously developed bimodal atomic force microscopy (AFM) based approach.[13] For each surface, the fouling experiments were conducted on three different samples, and on each sample the ellipsometry, XPS and AFM measurements were carried out at at least three different places. Fig. 2 shows the increased thickness of the four different surfaces after our fouling protocol determined from the attenuation of XPS signals of substrates in the presence of an overlayer (here: the fouling polymer). The increased thickness on the unmodified silicon and the **F1** and **F17** monolayers is determined by the increased atomic C/Si ratio,[27] while for the **PMAF17** brush the increased thickness can be calculated by the increased C/F ratio, since the fouling polymers do not contain any fluorine atom in the polymer chain. As a generic finding, the fouling polymer deposit on the **PMAF17** brush is <0.1 nm for both PS in toluene and P2VP in DMF. This result is evidently better than for those of unmodified Si, and the **F1** and **F17** monolayers, indicating that the as-prepared fluoropolymer brush exhibits superior antifouling properties towards the studied polymers. The best antifouling properties were achieved by the fluoropolymer brush due to its

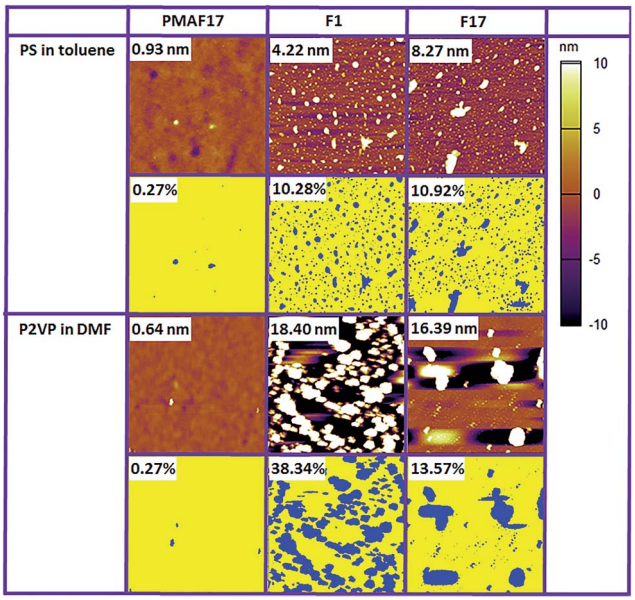

Fig. 3 Top: tapping mode AFM images (5 × 5 μm^2) in air of the **PMAF17** brush, **F1** and **F17** monolayers after 12 h immersion in polymer solution. Below: corresponding surface coverage of the modified surfaces assuming a threshold of 3 nm.

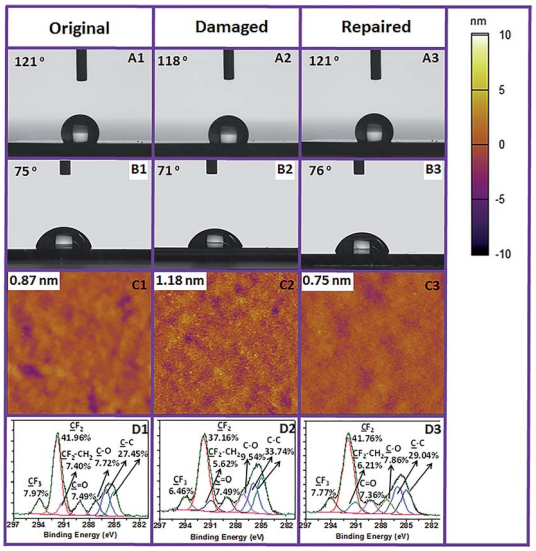

Fig. 4 Static contact angle (water: (A1–A3) and toluene: (B1–B3)), tapping-mode AFM image (C1–C3) and XPS carbon narrow scan (D1–D3) of the original, damaged and repaired **PMAF17** brush.

stronger hydrophobic interaction with the solvent compared with the references.

Surface morphology surveys of these surfaces by tapping mode AFM measurements further confirmed the polymer adsorption behavior. As shown in Fig. 3, after the fouling study, no polymer particles were found for the **PMAF17** brush, which further confirmed its superior antifouling properties towards polymers. In contrast, polymer particles are clearly observed on the **F1** and **F17** monolayers, resulting in higher roughness and confirming significant fouling of these monolayers under these conditions.

To determine the degree of fouling, we calculated the fraction of the surface that has a height (as determined by AFM) above a certain threshold value, and assumed that exceedance of this threshold value is the result of polymer fouling as the substrate is atomically flat and the polymer brush is smooth. The determined degree of fouling for the surfaces using a threshold value of 3 nm is shown in Fig. 3. Dark blue regions correspond to areas above the threshold, and are labelled as fouled by the polymer, while the yellow areas are classified as non-fouled areas. It can be clearly seen that for these two model systems, the fouled surface fraction of the **PMAF17** brush is by far the lowest (less than 0.3%) compared with that of **F1** and **F17** monolayers, further confirming its superior anti-fouling properties, in fact the **F1** and **F17** monolayers scored best as non-fouling coatings within a wide range of monolayers. The fouled surface fraction should, of course, decrease when increasing the threshold, but the variation from surface to surface does not vary substantially. The surface coverage on the **PMAF17** brush is always lowest irrespective of the precise threshold chosen (Fig. S2†). In addition, we also tested the anti-fouling properties of the **PMAF17** brush against some other polymers in different solvents (poly(acrylic acid) in methanol; poly(hydroxyl propyl methacrylate) in acetone; poly(4-chloro styrene) in ethyl acetate; polystyrene in dichloromethane; poly(adipic anhydride) in dimethylformamide; poly(*N*-isopropyl acrylamide) in trifluoroethanol). The AFM results in Fig. S3† illustrate that **PMAF17** brushes display excellent antifouling properties towards all these polymers studied.

Compared with monolayers, another advantage of the polymer brush is the long-term stability. In order to investigate the stability of our fluoropolymer brush under stringent conditions, we immersed the **PMAF17** brush into a swirling pH 11 solution for 24 h under standardized stability testing.[28] Subsequently, the surface was washed with water, ethanol and dichloromethane, dried with argon and then characterized by CA, AFM and XPS. The water and toluene static CA of this damaged brush were still 118° and 71° (Fig. 4A2 and B2), respectively, which illustrates that the fluoropolymer brush is highly stable in a basic environment, and that neither the polymer brush nor the attachment to the surface are significantly damaged. However, the 3° and 4° decrease in water and toluene static CA does indicate some polymer breakdown, which was confirmed by a slight increase of the surface roughness (Fig. 4C2). This increased surface roughness will likely also contribute to the relatively have wetting angle of the chemically degraded surface.

We hypothesized that above the T_g of the polymer brush (here: 40 °C)[29] the polymer chain might display sufficient mobility to reorient itself and reform an optimal surface. The driving force for this process should then be the low surface energy of the fluorinated materials,[30,31] which should cause undamaged fluorinated tails to come to the top of the surface during heating and repair the hydrophobicity and antifouling character of the surface. Indeed, and actually better than expected, the water and toluene static CA of the damaged polymer brush recovers to 121° and 76° after being heated at 120 °C for 2 h (Fig. 4A3 and B3). 120 °C was selected here because this temperature is far above the T_g of the fluorinated methacrylate,

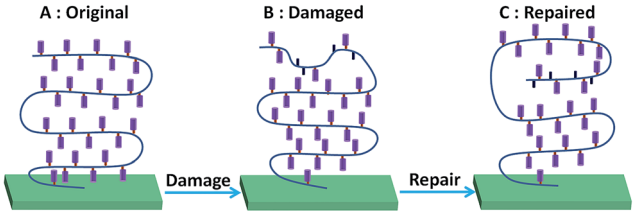

Fig. 5 Schematic illustration of the polymer segment orientation of the PMAF17 brush during the damage and repair process.

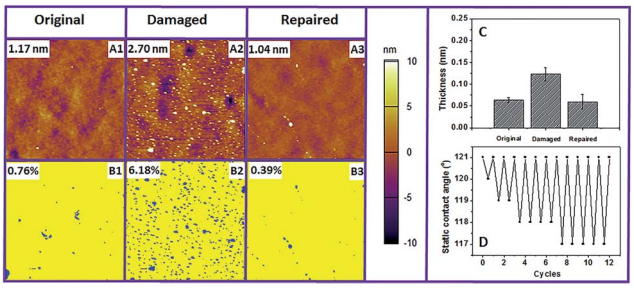

Fig. 6 (A1–A3) Tapping-mode AFM images of the original, damaged and repaired PMAF17 brushes after immersion into PS–toluene solution for 12 h, the inset value is AFM determined RMS. (B1–B3) Surface coverage of the original, damaged and repaired PMAF17 brushes after immersion into PS–toluene solution for 12 h, the inset value is the degree of fouling. (C) – The increased thickness determined by XPS of the original, damaged and repaired PMAF17 brushes after the fouling study in PS–toluene solution. (D) – The static contact angle changes of the PMAF17 brush between pH 11 1 h and 120 °C 2 h.

and thus allows facile chain reorientation. We noticed that, apart from the return of the hydrophobicity, also the original low RMS roughness also recovers (Fig. 4C3), together with regaining the original XPS spectra, specifically the C 1s XPS spectrum (see below). We thus hypothesize that, apart from reorientation of individual F_{17} side chains, the polymer backbone also rearranges. From studies of Takahara and co-workers it follows that C_8F_{17} chains in such a brush preferentially form a tightly packed structure due to the low surface free energy, where these side chains are oriented almost perpendicular to the substrate to afford a lamellar structure (Fig. 5A).[32] Based on the changes in the contact angle, increased polymer fouling, increased roughness and loss of F in the survey XPS spectrum, we reasoned that in addition to the loss of side chains during the damage process this molecular orientation is also partially lost, leading to *e.g.* a higher surface roughness (Fig. 5B). However, rearrangement of the polymer segments during heating will repair the top-layer molecular orientation (Fig. 5C) and the concomitant surface properties. The damaged brush hidden below may still influence the layer structure a bit, but will initially not influence the surface characteristics. Only upon further increased and repeated damage do these polymer reorientation processes not suffice anymore, and more permanent damage results.

To confirm that these molecular reorientation processes are indeed responsible for the damage–repair process, detailed XPS studies were performed. Fig. 4D1–D3 shows the C 1s narrow scan of the original, damaged and repaired fluoropolymer brush. The initial fraction of C atoms connected to fluorine is 57.3%, which is close to the theoretical value (57.1%; 8 out of the 14 C atoms in the monomer). The C 1s XPS data clearly show that this value decreases to 49.2% upon alkaline damage, suggesting partial loss of fluorinated tails by basic hydrolysis of the ester group in the polymer backbone. This ratio recovers to 55.7% after heating, *i.e.* close to the initial value. We interpret this as that the carboxylic acid groups that are formed during the hydrolysis process are buried again by the regenerated top-layer fluorinated tail induced by the rearrangement of the polymer segments during heating. This damage–repair cycle of hydrophobicity can be repeated many times (Fig. 6D). The overall thickness of the **PMAF17** brush decreased significantly after 12 damage–repair cycles, from 75 nm to 43 nm (Table S2†). In line with the continuing accumulation of carboxylic acid moieties, the SCA decreases more dramatically after several alkaline treatments, but still the surface hydrophobicity and smoothness can be completely repaired. Apart from stability in a basic environment, the **PMAF17** brush also possesses good stability in acidic media and under UV exposure. The water static CA only decreases to 116° and 119° at pH 3 for 24 h, and under UV (254 nm, 3 cm above the sample) exposure for 1 h, respectively. The CA of these damaged brushes in these two cases also recovers to the same values as the freshly prepared ones after heating at 120 °C for 2 h (Table S3 and S4†). It is worth mentioning here that our surfaces can also be repaired several times in an acidic environment or under UV exposure. Here we only took a basic environment as a typical damage condition to investigate the molecular event responsible for the damage–repair process and antifouling properties of the brushes after self-healing, as the acid conditions or UV irradiation are typically less damaging for these surfaces, and base-induced damage thus displays the regeneration potential of the polymers under study most clearly.

Next, the polymer fouling behavior on the original, damaged and repaired fluoropolymer brushes was investigated by AFM and XPS. Here we used PS in toluene as a model system. As described above, the originally prepared brush displays excellent anti-fouling behavior (Fig. 6A1 and B1), while heavy fouling was observed on the surface damaged at pH 11 for 24 h (Fig. 6A2 and B2). Such heavy fouling was confirmed by polymer particles that could be found on the surface. And also the RMS surface roughness and the fouled surface fraction of the damaged brush increase dramatically compared with the freshly prepared brush [original RMS and surface coverage: 1.17 nm and 0.76%; RMS and surface coverage after damage: 2.70 nm and 6.18%]. In contrast, upon heating of a damaged surface at 120 °C for 2 h and cooling down, immersion of the resulting repaired surface into a fouling polymer solution did not yield any remaining fouling polymer particles after rinsing. Furthermore, the repaired surface also achieves the same surface roughness and fraction of surface fouling as the freshly prepared one (Fig. 6A3 and B3). In addition, the XPS results determined by the atomic C/F ratio after the fouling study exhibit the same trend as we obtained from the AFM measurements (Fig. 6C). These

observations indicate that basically no fouling happens on the repaired fluoropolymer brush, which illustrates that the repaired **PMAF17** brush displays the same highly favorable antifouling behavior as the undamaged one. We attribute the intermediate fouling upon damage of the brush to the reduced surface oleophobicity, which results from the hydrolysis of some ester bonds to carboxylates as also confirmed by XPS (see Fig. 4 D2 *versus* D1 and D3).

In summary, a highly polymer-repellent fluoropolymer brush with excellent stability in a basic/acidic environment or under UV exposure was successfully prepared by surface-initiated ATRP. Upon damage in basic/acidic media or under UV exposure, the hydrophobicity and antifouling character of the brush can simply be repaired many times by heating. It is likely that this type of chemistry can be combined with *e.g.* micro- and nano-structuring and other advanced materials properties to yield even better long-term antifouling behavior under harsh environments.[33–36] Studies on the influence of the molecular architecture and degree of fluorination on the self-healing and antifouling properties are currently ongoing in our lab.

Acknowledgements

This research was carried out under project number M62.3.12453 in the framework of the Research Program of the Materials innovation institute M2i (http://www.m2i.nl).

Notes and references

1 C. Blaszykowski, S. Sheikh and M. Thompson, *Chem. Soc. Rev.*, 2012, **41**, 5599–5612.
2 A. J. Scardino and R. de Nys, *Biofouling*, 2011, **27**, 73–86.
3 N. Fusetani, *Nat. Prod. Rep.*, 2004, **21**, 94–104.
4 I. Banerjee, R. C. Pangule and R. S. Kane, *Adv. Mater.*, 2011, **23**, 690–718.
5 K. L. Prime and G. M. Whitesides, *Science*, 1991, **252**, 1164–1167.
6 S. Y. Jiang and Z. Q. Cao, *Adv. Mater.*, 2010, **22**, 920–932.
7 Q. Shao and S. Y. Jiang, *Adv. Mater.*, 2015, **27**, 15–26.
8 P. Saikhwan, J. Y. M. Chew, W. R. Paterson and D. I. Wilson, *Ind. Eng. Chem. Res.*, 2007, **46**, 4846–4855.
9 A. P. Watkinson, *Chem. Eng. Technol.*, 1992, **15**, 82–90.
10 T. E. Bockstahler and C. R. Hunt, *US*3705190 A, 1972.
11 D. M. Mcfadden and R. S. H. Wu, *EP*1024149 B1, 2000.
12 J. C. Kuschnerow, S. Dorn, H. Föst, W. Augustin and S. Scholl, *Proceedings of International Conference on Heat Exchanger Fouling and Cleaning*, 2013, pp. 150–157.
13 Z. Wang, S. P. Pujari, B. Lagen, M. M. J. Smulders and H. Zuilhof, *Adv. Mater. Interfaces*, 2016, 201500514.
14 Y. Yang and M. W. Urban, *Chem. Soc. Rev.*, 2013, **42**, 7446–7467.
15 M. D. Hager, P. Greil, C. Leyens, S. van der Zwaag and U. S. Schubert, *Adv. Mater.*, 2010, **22**, 5424–5430.
16 Z. H. Wang, Y. Yang, R. Burtovyy, I. Luzinov and M. W. Urban, *J. Mater. Chem. A*, 2014, **2**, 15527–15534.
17 T. S. Wong, S. H. Kang, S. K. Y. Tang, E. J. Smythe, B. D. Hatton, A. Grinthal and J. Aizenberg, *Nature*, 2011, **477**, 443–447.
18 H. Kuroki, I. Tokarev, D. Nykypanchuk, E. Zhulina and S. Minko, *Adv. Funct. Mater.*, 2013, **23**, 4593–4600.
19 D. D. Chen, M. D. Wu, B. C. Li, K. F. Ren, Z. K. Cheng, J. Ji, Y. Li and J. Q. Sun, *Adv. Mater.*, 2015, **27**, 5882–5888.
20 L. Li, B. Yan, J. Q. Yang, L. Y. Chen and H. B. Zeng, *Adv. Mater.*, 2015, **27**, 1294–1299.
21 Q. Wei, C. Schlaich, S. Prevost, A. Schulz, C. Bottcher, M. Gradzielski, Z. H. Qi, R. Haag and C. A. Schalley, *Adv. Mater.*, 2014, **26**, 7358–7364.
22 D. Borisova, D. Akcakayiran, M. Schenderlein, H. Mohwald and D. G. Shchukin, *Adv. Funct. Mater.*, 2013, **23**, 3799–3812.
23 N. S. Bhairamadgi, S. P. Pujari, C. J. M. van Rijn and H. Zuilhof, *Langmuir*, 2014, **30**, 12532–12540.
24 J. Tsibouklis and T. G. Nevell, *Adv. Mater.*, 2003, **15**, 647–650.
25 S. Yamamoto, Y. Tsujii and T. Fukuda, *Macromolecules*, 2002, **35**, 6077–6079.
26 L. Singh, P. J. Ludovice and C. L. Henderson, *Thin Solid Films*, 2004, **449**, 231–241.
27 L. Scheres, M. Giesbers and H. Zuilhof, *Langmuir*, 2010, **26**, 4790–4795.
28 N. S. Bhairamadgi, S. P. Pujari, F. G. Trovela, A. Debrassi, A. A. Khamis, J. M. Alonso, A. A. Al Zahrani, T. Wennekes, H. A. Al-Turaif, C. van Rijn, Y. A. Alhamed and H. Zuilhof, *Langmuir*, 2014, **30**, 5829–5839.
29 T. Yamashita, H. Miyauchi, Y. Kawarada, K. Nakamura and N. Oishi, CA 2297159, 2003.
30 A. C. C. Esteves, Y. Luo, M. W. P. van de Put, C. C. M. Carcouet and G. de With, *Adv. Funct. Mater.*, 2014, **24**, 986–992.
31 T. Dikic, W. Ming, R. van Benthem, A. C. C. Esteves and G. de With, *Adv. Mater.*, 2012, **24**, 3701–3704.
32 H. Yamaguchi, K. Honda, M. Kobayashi, M. Morita, H. Masunaga, O. Sakata, S. Sasaki and A. Takahara, *Polym. J.*, 2008, **40**, 854–860.
33 H. X. Wang, Y. H. Xue, J. Ding, L. F. Feng, X. G. Wang and T. Lin, *Angew. Chem., Int. Ed.*, 2011, **50**, 11433–11436.
34 Y. Li, L. Li and J. Q. Sun, *Angew. Chem., Int. Ed.*, 2010, **49**, 6129–6133.
35 C. H. Xue and J. Z. Ma, *J. Mater. Chem. A*, 2013, **1**, 4146–4161.
36 C. H. Xue, Z. D. Zhang, J. Zhang and S. T. Jia, *J. Mater. Chem. A*, 2014, **2**, 15001–15007.

